Civil Engineering Dimension
https://ced.petra.ac.id

Finite Element Analysis of The Effect of Fiber Content on The Flexural Strength of SFRC Beams with Steel Rebars

Nurhuda, I.[1]*, Prasetya, B.H.[1], Nuroji[1], and Priastiwi, Y.A.[1]
[1] Diponegoro University, Jl. Prof. Soedarto, SH., Tembalang, Semarang 50275, INDONESIA

DOI: https://doi.org/10.9744/ced.26.2.101-110

Article Info:
Submitted: Apr 04, 2024
Reviewed: Jul 12, 2024
Accepted: Aug 08, 2024

Keywords:
finite element,
fiber content,
steel fiber,
RC beams,
flexural strength,
crack pattern.

Corresponding Author:
Nurhuda, I.
Diponegoro University, Jl. Prof. Soedarto, SH., Tembalang, Semarang 50275, INDONESIA
Email: ilham@live.undip.ac.id

Abstract

This research aimed at studying the effect of fiber content on the flexural strength and behavior of steel fiber reinforced concrete (SFRC) beams with steel rebars. The study employed finite element (FE) analysis to simulate the behavior of SFRC beams. The simulation results of the FE model were validated against experimental data. Subsequently, the validated model was utilized to analyze the strength and crack patterns of SFRC beams with steel rebars in comparison to conventional RC concrete beams without fibers. The parametric study indicates an average 9% increase in RC beam capacity for every 1% increment in fiber volume fraction. Moreover, this study reveals more substantial effects of steel fibers on beams with low reinforcement ratios. Crack analysis shows that cracks in the SFRC beams are distributed more evenly compared to plain RC beams at regions with the same bending moment, indicating enhanced strength to sustain loads, reduced deflection, and improved beam ductility.

Introduction

Steel fiber reinforced concrete (SFRC) has been widely used in the construction industry for various types of structures [1]. The increasing popularity of SFRC is attributed to its superior mechanical properties compared to plain concrete without fibers. Research has shown that the addition of steel fibers to concrete enhances its tensile strength, crack resistance, and reduces crack widths in structures [2–5]. Moreover, SFRC exhibits improved compressive strength [6–8], shear strength [9,10], flexural strength [7,11], and impact resistance [12–14]. Furthermore, SFRC reduces creep in concrete, making it particularly suitable for prestressed concrete structures, mitigating stress loss due to creep [15,16].

The distinctive material behavior of SFRC compared to plain concrete significantly influences the performance of SFRC-based structures. When SFRC is applied to flexural elements, it reduces the need for compressive reinforcement while preserving ductility [17,18]. SFRC beams demonstrate higher ultimate loads and better resistance to shear forces than beams made with plain concrete [19,20]. Additionally, the use of SFRC in beams improves their resistance to strength degradation under cyclic loading conditions [11].

Previous research generally indicates an increase in load-carrying capacity in SFRC beams compared to those made with plain concrete. However, the magnitude of this strength enhancement and the influence of fiber percentage on the percentage increase in beam strength have not been thoroughly investigated. Furthermore, the effect of fiber content on crack patterns in beams remains largely unexplored.

The finite element method (FEM) is commonly employed to analyze reinforced concrete structures. However, its use in SFRC structures remain limited. Abbas *et al*. [21] conducted 3D FEM analysis of SFRC beams using ABAQUS,

Note : Discussion is expected before November, 1st 2024, and will be published in the "Civil Engineering Dimension", volume 27, number 1, March 2025.
ISSN : 1410-9530 print / 1979-570X online
Published by : **Petra Christian University**

while Beshara [22] employed ANSYS software. Although 3D FEM models provided simulation results that closely matched laboratory tests, the complexity of modeling and longer processing times are drawbacks of 3D FEM models. Several studies have utilized 2D FEM for the analysis of SFRC. For instance, Campione [23] employed FEM in conjunction with the ATENA software to investigate the behavior of SFRC beams. In Campione's model, the beams were represented using 9-node shell elements, and the behavior of the concrete material was defined through a constitutive model. Campione's model yielded results that exhibited a strong correlation with experimental data obtained from flexural and deep beams [24].

Campione [23] utilized a stress-strain relationship to model the tensile behavior of steel fiber-reinforced concrete. It was assumed in the model that, after reaching the maximum tensile stress, the stress dropped to a constant residual value. However, no ultimate tensile strain was specified in the model.

This paper enhances the material models used in Campione's study [23] by explicitly specifying the ultimate strain in the material model. The modified model is then incorporated into a 2D FEM model of SFRC beams with steel rebars, and the results are calibrated against laboratory test data. The calibrated model is subsequently employed to simulate the effect of steel fiber volume fraction on beam strength and crack patterns.

Modelling of SFRC Beams

Finite Element Modelling and Analysis

The SFRC beams were modeled in 2D using DIANA FEA software [25]. Plane elements were employed to model the fiber-reinforced concrete section of the beams. The chosen plane elements were isoparametric quadrilaterals of plane stress type with 8 nodes. The reinforcement was modeled using line elements, where truss elements were used for embedded reinforcement and beam elements for reinforcement with bond slip.

The concrete material was represented by constitutive equations for both compression and tension conditions. Cracking in concrete was modeled using the smeared crack model, and the failure of concrete elements was analyzed based on total strain-based crack models [26] with the crack direction modeled as a fixed crack [25]. The steel material was represented by a tri-linear model for tension and compression conditions.

The finite element mesh was studied using mesh sizes of 20 mm, 10 mm, and 5 mm. The optimal mesh size was determined using sensitivity tests. Nonlinear analysis was performed using the Quasi-Newton method. Convergence criteria were set based on energy, force, or deformation, and once any one of these criteria was satisfied, the analysis was considered converged.

Constitutive Equation for SFRC in Compression

Nataraja *et al*. [6] studied the effect of steel fibers on concrete with compressive strengths ranging from 30 MPa to 50 MPa, and steel fiber content (v_f) ranging from 0.5% to 1% of the concrete volume. Each percentage was further divided into two aspect ratios (l/d), namely 55 and 82. The relationship between compressive strength and steel fiber variables was expressed proportionally with the reinforcing index (RI), which depended on the fiber content in percentage by weight and the aspect ratio (l/d) of the fibers, as shown in Equation (1). Campione & Mangiavillano [11] also adopted Equation (1) to analyze SFRC beams under monotonic and cyclic loading. Similar formulas were presented by Thomas & Ramaswamy [8] and Abbass [27], but with different constant values in the equation. This study used the equation employed by Nataraja *et al*. [6], as shown in Equation (1).

$$f_{cf} = f_c' + 2.1604 \cdot RI \quad (1)$$

where f_{cf} is compressive strength of fiber-reinforced concrete (MPa), fc' is compressive strength of plain concrete at 28 days (MPa), RI is reinforcing index ($= w_f \times (l/d)$), l is fiber length (mm), d is fiber diameter(mm), and w_f= weight percentage of fibers per m^3. Weight percentage of fiber (w_f) is approximately equal to 3.2 times the fiber content (v_f). The relationship between the maximum compressive strength of fiber-reinforced concrete, f_{cf}, and the corresponding strain at maximum compressive strength (ε_{of}) can be calculated using Equation (2) [28] and adopted in this study. The compressive strain of fiber-reinforced concrete at the ultimate condition (ε_{uf}) is also known to be greater than the ultimate strain of plain concrete. Lok and Xiao [29] proposed a value of 0.0038 for the ultimate compressive strain of fiber-reinforced concrete with fiber content ranging from 0.5% to 2.0%. Additionally, the addition of fibers to concrete enhances the elastic modulus of concrete. Thomas & Ramaswamy [8] suggested that the elastic modulus of fiber-reinforced concrete can be computed using Equation (3).

$$\varepsilon_{of} = 0.00076 + \sqrt{(0.626 \cdot f_{cf} - 4.33) \cdot 10^{-7}} \quad (2)$$

$$E_{cf} = 4.58 \cdot (f_c')^{0.5} + 0.13 \cdot (f_c') \cdot RI + 0.12 \cdot RI \quad (3)$$

where ε_{of} is strain at maximum compressive strength, E_{cf} is elastic modulus of fiber-reinforced concrete (GPa).

The maximum compressive stress of fiber-reinforced concrete (f_{cf}), the elastic modulus of fiber-reinforced concrete (E_{cf}), the strain at maximum compressive stress (ε_{of}), and the ultimate compressive strain of fiber-reinforced concrete (ε_{uf}) are used to formulate the stress-strain equation for fiber-reinforced concrete. The stress-strain relationship up to the maximum compressive stress tends to follow a parabolic curve [30] and can be modeled by Equation (4). The softening behavior after the maximum compressive stress is modeled using Equation (5) based on Popovics [31], which is applicable to both normal and high-strength concrete.

$$f_c = -f_{cf}\left(2 \cdot \frac{\varepsilon}{\varepsilon_{of}} - \left(\frac{\varepsilon}{\varepsilon_{of}}\right)^2\right); 0 < \varepsilon \leq \varepsilon_{of} \quad (4)$$

$$f_c = -f_{cf}\frac{n_c \cdot \left(\frac{\varepsilon}{\varepsilon_{of}}\right)}{n_c - 1 + \left(\frac{\varepsilon}{\varepsilon_{of}}\right)^{n_c}} \; ; \; n_c = \frac{E_{cf}}{E_{cf} - \frac{f_{cf}}{\varepsilon_{of}}} \; ; \; \varepsilon > \varepsilon_{of} \quad (5)$$

where f_c is compressive stress at a certain strain (MPa), and ε is compressive strain.

Constitutive Modelling of SFRC in Tension

The enhancement of tensile strength is one of the primary objectives of adding fibers to concrete. Mathematical models describing the influence of fiber addition on the tensile strength of concrete have been reported in several references [8,21,29,32,33]. This study adopts Equation (6) from Thomas & Ramaswamy [8] to represent the effect of fiber addition on the tensile strength of concrete. The addition of fibers to concrete not only increases its maximum tensile strength but also provides post-cracking tensile strength [22]. Equation (7) is used to calculate the residual tensile strength of SFRC.

$$f_{tf} = 0.63 \cdot (f_c')^{0.5} + 0.09 \cdot (f_c')^{0.5} \cdot RI + 0.017 \cdot RI \quad (6)$$

$$f_{tr} = 0.09 \cdot RI \cdot (f_{cf})^{2/3} \quad (7)$$

where f_{tf} is tensile strength of fiber-reinforced concrete (MPa), and f_{tr} is residual tensile strength of fiber-reinforced concrete (MPa).

The stress-strain relationship of fiber-reinforced concrete under tension can be represented as shown in Figure 1. The strain at maximum tensile stress (ε_{tf}) is proposed by Abdul-Razzak and Mohammed Ali [34] in Equations (8)-(9) based on the research data of Lin et al. [35]. The strain ε_{tr} at which the tensile stress reduces to the residual tensile strength is calculated using Equations (10)-(11) as proposed by Lok & Xiao [29] and Kim et al. [36].

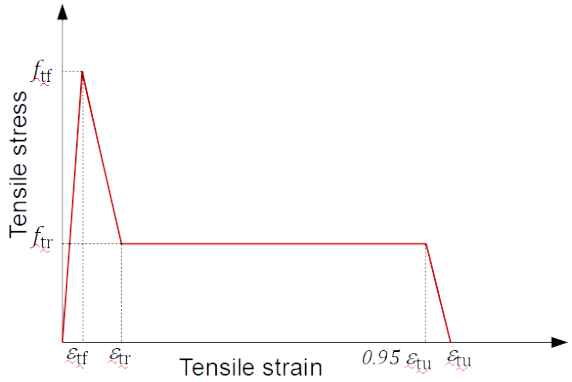

Figure 1. Stress-strain Relationship Model under Tension Conditions

$$\varepsilon_{tf} = \varepsilon_t + 0.00026 \cdot N_f \cdot l \cdot d \quad (8)$$

$$N_f = \beta \cdot \left(\frac{4 \cdot V_f}{\pi \cdot d^2}\right) \quad (9)$$

$$\varepsilon_{tr} = \tau_d \cdot \frac{l}{d} \cdot \frac{1}{E_{sf}} \quad (10)$$

$$\tau_d = 2.5 \cdot f_t \text{ for hooked steel fibers} \quad (11)$$

where ε_{tf} is strain at the maximum stress of fiber-reinforced concrete, ε_t is strain at the maximum tensile stress of plain concrete, v_f is fiber volume fraction (%), β is fiber orientation factor, ε_{tr} is residual strain of tensile stress of fiber-reinforced concrete, E_{sf} is fiber elastic modulus (MPa), f_t is tensile strength of plain concrete (MPa), and τ_d is fiber bond strength (MPa). Fiber bond strength for different shapes of steel fibers are available in the literature [36]. The influence of fibers on the ultimate tensile strain, ε_{tu}, has been reported in several literature sources [21,37]. In those studies, the ultimate tensile strain, ε_{tu}, of fiber-reinforced concrete was found to be approximately 2-2.5%. However, Tlemat *et al*. [38] indicates that a high fiber volume fraction can increase the ultimate tensile strain by up to 4%. This research employed a linear equation to estimate the ultimate strain of fiber-reinforced concrete at fiber volume fractions ranging from 0.01% to 2%, as given in Equations (12)–(13).

$$\varepsilon_{tu} = 2 \cdot v_f \; ; \; 0.01\% < v_f < 2\% \tag{12}$$

$$\varepsilon_{tu} = 0.04 \; ; \; v_f \geq 2\% \tag{13}$$

Constitutive Modeling of Steel Rebars and Bond-slip between Rebars and Concrete

The stress-strain relationship of steel reinforcements is modeled as tri-linear. The material properties used as inputs include the elastic modulus of steel reinforcements (E_s), yield stress (f_y), maximum stress (f_u), strain at maximum stress (ε_{sm}), and ultimate strain (ε_{SU}). The steel stress beyond reaching the maximum stress is modeled as constant up to its ultimate strain. The bond-slip behavior between reinforcement and concrete is characterized using the tension-slip relationship according to the fib Model Code 2010 [39].

Method

The research was conducted through the following stages: finite element model creation and validation against experimental results, parametric study using FE analysis, discussion, and conclusion.

Modeling and Validation against Experimental Data

The comparison between FEM analysis and experimental testing was carried out using the experimental data of SFRC beams conducted by Oh *et al*. [40], which can be found in the literature. The test specimens were beams with dimensions of 100 × 180 × 1700 mm and a span length of 1300 mm, as shown in Figure 2. The beams were reinforced with flexural and shear reinforcement. The properties of the reinforcement, stirrup spacing, fiber percentage, compressive strength of fiber-reinforced concrete (f_{cf}), splitting tensile strength of fiber-reinforced concrete (f_{SP}), and other material properties are presented in Tables 1 and 2. The steel fibers used had a length of 42 mm and a fiber diameter of 0.7 mm with an aspect ratio of l/d = 60. For validation purposes, data from two beams with a shear reinforcement ratio of 0.75 were used, where one beam was made with plain concrete, and the other beam was made with concrete containing 1% volume fraction of fibers.

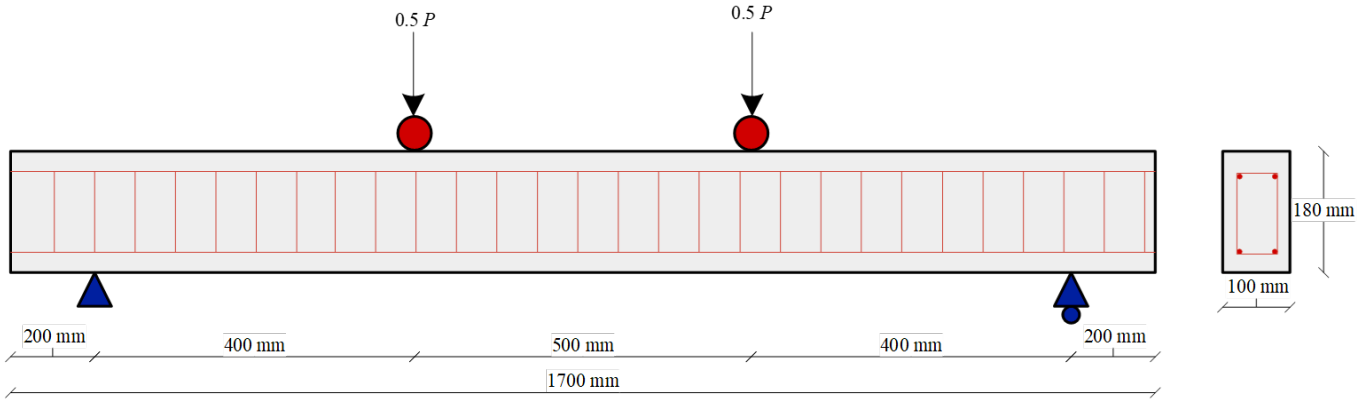

Figure 2. Tested Beam [40]

Tabel 1. Details of the Tested Beams

Beam	Stirrup		Fibers		f_{cf}(MPa)	f_{SP} (MPa)
	Spacing (mm)	□v	Aspect ratio, *l*/*d*	v_f (%)		
S0.75V0	60	0.009	60	0	34.0	2.5
S0.75V1	60	0.009	60	1	38.7	4.0

Tabel 2. Material Properties of the Steel Bars and Steel Fibers

	Yield strength (MPa)	Tensile strength (MPa)	Modulus of elasticity (MPa)
Longitudinal steel	420	545	2 x 10^5
Stirrup	359	534	2 x 10^5
Steel fiber	1303	1784	2 x 10^5

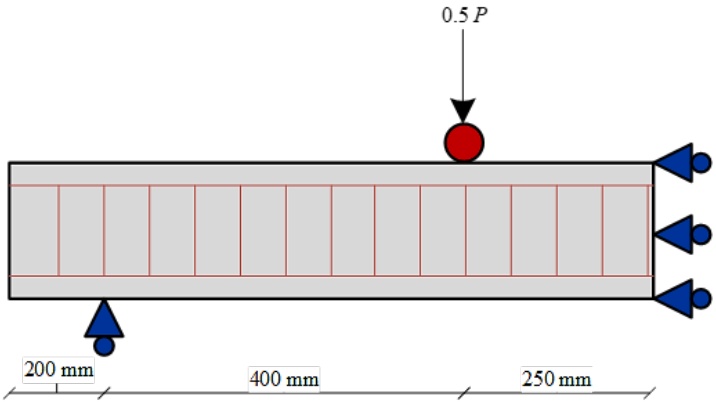

Figure 3. Half-span Model in FE Analysis

Finite element analysis was performed for a half-span as shown in Figure 3. Sensitivity analysis was conducted by varying the mesh size from 5 mm (6974 elements), 10 mm (1820 elements), to 20 mm (470 elements). This sensitivity analysis aimed to examine the maximum load and maximum deflection obtained from the FEM analysis and compare them with the results of experimental testing.

Parametric Study

The verified model from experimental results is used for further analysis. A parametric study is conducted to investigate the influence of fiber content on the behavior of beams with different tensile reinforcement ratios. There are 4 variations of tensile reinforcement ratio (ρ) considered: 0.0149, 0.0173, 0.0221, and 0.0245. Each beam with the same tensile reinforcement ratio is analyzed with 3 different fiber contents (v_f): 0%, 1%, and 2%. The details of the tensile reinforcement ratio of the beams and their fiber contents can be found in Table 3.

Tabel 3. Reinforcement Ratio and Fiber Content of the Studied Beams

Specimens	ρ (%)	A_s (mm^2)	V_f (%)
B-1.49-V-0	1.49	213.840	0
B-1.49-V-1	1.49	213.840	1
B-1.49-V-2	1.49	213.840	2
B-1.73-V-0	1.73	248.590	0
B-1.73-V-1	1.73	248.590	1
B-1.73-V-2	1.73	248.590	2
B-2.21-V-0	2.21	318.088	0
B-2.21-V-1	2.21	318.088	1
B-2.21-V-2	2.21	318.088	2
B-2.45-V-0	2.45	352.837	0
B-2.45-V-1	2.45	352.837	1
B-2.45-V-2	2.45	352.837	2

Results and Discussion

Influence of Mesh Size

The comparison between FEA results with different mesh sizes and experimental results shows that all mesh sizes used for the test specimens without fiber provide close estimates of the ultimate load, with a maximum ratio between the maximum load from simulation and physical tests of 1.04. The deflection analysis reveals that Finite Element (FE) models of Reinforced Concrete (RC) beams with fibers offer more accurate predictions than those without fibers. The ratios of maximum deflection from simulation to physical test results are consistently close to 1 across various element variations. Conversely, FE models of RC beams without fibers, with mesh sizes of 10 mm (1820

elements) and 20 mm (470 elements), yield significantly higher predictions of maximum displacement compared to experimental results. However, the FE model without fibers, featuring a 5 mm mesh size (6974 elements), provides a much closer prediction to the experimental results.

Based on the results of the maximum load and deflection analyses, FE models with a 5 mm mesh size were employed for the plain RC beam models, and a 10 mm mesh size was used for the fiber-reinforced concrete models to ensure accurate analysis results.

The Influence of Fiber Content on Load-displacement Relationship

The load-displacement relationship of beams with different fiber content and tensile reinforcement ratios was obtained through numerical simulations using the selected model as mentioned earlier. Figs. 4(a) – 4(d) show the load-displacement relationships of beams with the same tensile reinforcement ratio but varying fiber percentages. Generally, the addition of steel fibers increases the maximum load by approximately 9 % for each 1% increase in fiber content.

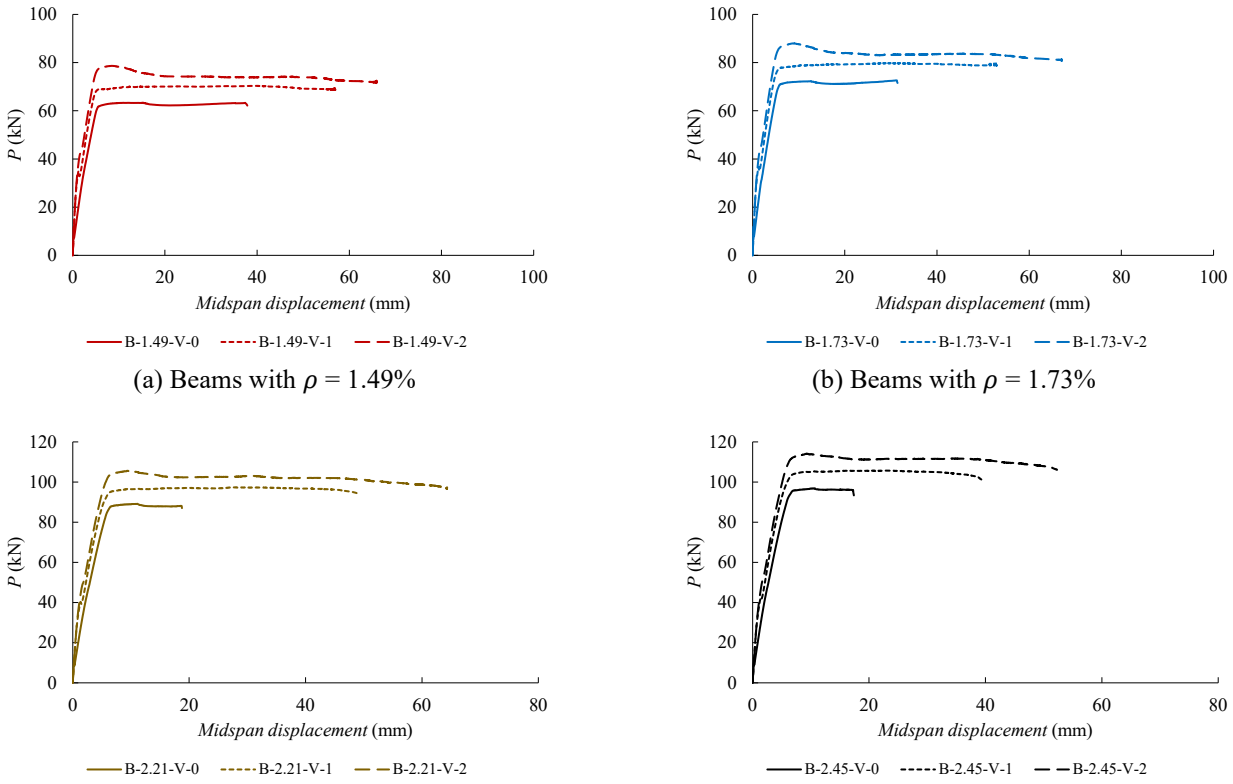

(a) Beams with ρ = 1.49%

(b) Beams with ρ = 1.73%

(c) Beams with ρ = 2.21%

(d) Beams with ρ = 2.45%

Figure 4. Load-deflection of Beams with Different Reinforcement Ratios (ρ) and Fiber Volume Fraction

Figure 4 illustrates the influence of fiber content on the load-displacement relationship of beams. It is evident that an increase in the fiber content enhances both the maximum load and the maximum deflection in beams with the same tensile reinforcement ratio. This observation aligns with the findings of Campione [23,24], which demonstrated an increase in the maximum load for fiber reinforced beams compared to plain RC beams. Furthermore, Figure 5 illustrates that, in addition to enhancing the flexural capacity of beams, an increased fiber content also leads to improved beam ductility. This enhancement in ductility is attributed to the effective bonding between the fibers and the concrete at crack locations, enabling the beams to maintain their strength even after cracking occurs [4]. The increase in ultimate displacement, however, is closely tied to the bonding strength between fibers and concrete. A study by Kim, K.S. *et al*. [36] has demonstrated that hooked fibers, such as those used in this research, exhibit superior bonding strength when compared to other types of steel fibers. As a result, the increase in ultimate displacement observed in this simulation can be regarded as a maximum estimate.

The increase in the maximum load at the ultimate condition is illustrated in Figure 5. For beams with the same reinforcement ratio, the load increase ranged from 7.1% to 11.7%, averaging 9.2% per 1% fiber content. The primary reason for this boost in the maximum load at the ultimate condition was the contribution of steel fibers in resisting

the tensile stresses occurring in the beams. According to research by Barros *et al*. [37], steel fiber-reinforced concrete can endure substantial strains, explaining the observed increase in load. As shown in Figure 5, the contribution of steel fibers to the load-carrying capacity of beams is more significant in those with lower reinforcement ratios. Further analysis reveals that steel fiber can effectively replace the minimum reinforcement ratio.

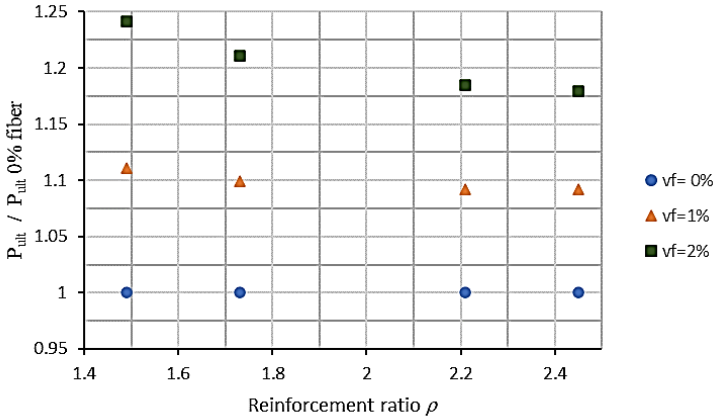

Figure 5. The Increment of Ultimate Load in SFRC Beams with Varied Reinforcement Ratio (ρ) and Steel Fiber Volume Fraction (v_f)

Crack Pattern

RC Beams without Fibers

The crack pattern provides information about the type of failure that occurs in the structure. Cracking in beams under bending conditions usually initiates with vertical cracks at the location of maximum moment. Subsequently, diagonal cracks may appear from the support towards the load location, depending on the shear strength of the beam and the aspect ratio (a/d). In this study, the shear reinforcement in the beams was provided at 0.75 of the required shear reinforcement for plain RC beams, with an aspect ratio (a/d) of 2.67.

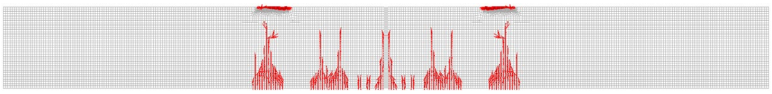

(a) Crack Pattern at Load P = 25% P_{ult}

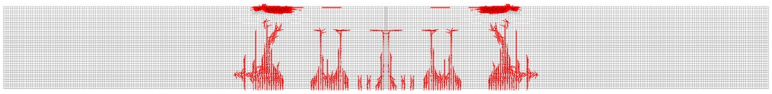

(b) Crack Pattern at Load P = 50% P_{ult}

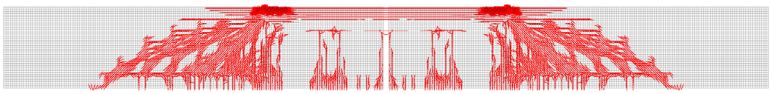

(c) Crack Pattern at Load P = P_{ult}

Figure 6. Crack Pattern in Plain RC Beams from FE Analysis

Simulation using the finite element method reveals the crack initiation stages in the beam. The FEM model represents a half-span symmetrical beam. Figure 6(a) illustrates the simulation results of the crack pattern in the beam at a load range of 25% of the ultimate load. At this stage, cracks occur in the middle of the beam span, where the maximum moment is present. Cracking continues in the middle region of the beam until the load reaches 50% of the ultimate load, as depicted in Figure 6(b). Subsequently, diagonal cracks start to appear, as shown in the final stage of the beam in Figure 6(c), demonstrating consistency with results from experimental testing in the laboratory [40].

Steel Fiber RC Beams

Steel fiber-reinforced concrete beams with steel rebars exhibit a different crack pattern compared to concrete without fibers, as shown in Figure 7. The distribution of fibers in the concrete provides more uniform additional strength to the beam in resisting tensile stresses, resulting in an overall increase in beam strength.

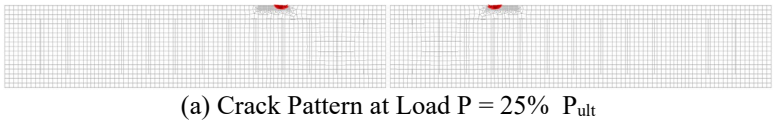

(a) Crack Pattern at Load P = 25% P_{ult}

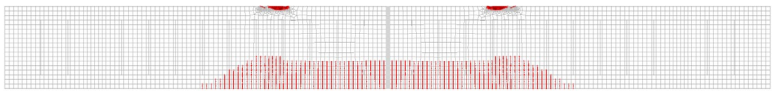

(b) Crack Pattern at Load P = 50% P_{ult}

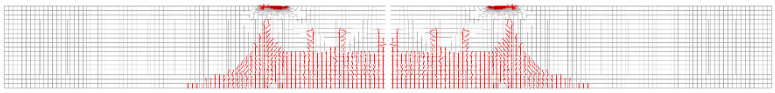

(c) Crack Pattern at Load P = P_{ult}

Figure 7. Crack Pattern in SFRC Beams with Steel Rebars from FE Analysis

The influence of fiber distribution leads to a more evenly distributed tensile strength in the beam. Cracks are more evenly distributed in the flexural region of the beam, as shown in Figure 7(b). Additionally, the presence of fibers is known to enhance the shear strength of the beam [22,41]. This is evident in Figure 7(c), where no diagonal cracks are present in the beam, as observed in the case of beams without fibers.

The use of steel fiber-reinforced concrete beams can reduce structural cracking under low loading conditions, and the ability of steel fibers to bridge the cracks can decrease the magnitude of structural deformation, as illustrated in Figure 4. At the same load level, steel fiber-reinforced concrete beams exhibit smaller deformations compared to plain reinforced concrete beams without fibers.

Conclusions

Numerical studies using the finite element method in this research resulted in the following conclusions:

1. The proposed tensile stress-strain relationship as presented in Equations (6)–(13), which includes the consideration of ultimate strain, effectively simulates the ultimate behavior of SFRC beams.
2. The addition of steel hooked fibers increases both the flexural strength and maximum deflection of SFRC beams with steel rebars.
3. The flexural strength of the beams increases by approximately 9% for each 1% increase in fiber volume fraction (v_f). The maximum fiber volume fraction studied in this research is 2%. The use of fiber content higher than 2% requires further investigation.
4. The effect of steel fibers on the load carrying capacity of SFRC beams is more pronounced on beams with low reinforcement ratios.
5. The addition of fibers leads to delayed cracking in the beams and a more uniform distribution of cracks compared to beams without fibers. Additionally, the presence of steel fibers restrains crack propagation and widening, resulting in increased stiffness and ductility of the beams.

References

1. Vijayan, D.S., et al., A Comprehensive Analysis of the Use of SFRC in Structures and Its Current State of Development in the Construction Industry, *Materials*, *15*(19), 2022, pp. 1-25.
2. Altun, F., Haktanir, T., and Ari, K., Effects of Steel Fiber Addition on Mechanical Properties of Concrete and RC Beams, *Construction and Building Materials*, *21*(3), 2007, pp. 654–661.
3. Soulioti, D.V., Barkoula, N.M., Paipetis, A., and Matikas, T.E., Effects of Fibre Geometry and Volume Fraction on the Flexural Behaviour of Steel-fibre Reinforced Concrete, *Strain*, *47*, 2011, pp. 535–541.
4. Soutsos, M.N., Le, T.T., and Lampropoulos, A.P., Flexural Performance of Fibre Reinforced Concrete Made with Steel and Synthetic Fibres, *Construction and Building Materials*, *36*, 2012, pp. 704–710.
5. Wang, Z.L., Wu, J., and Wang, J.G., Experimental and Numerical Analysis on Effect of Fibre Aspect Ratio on Mechanical Properties of SRFC, *Construction and Building Materials*, *24*(4), 2010, pp. 559–565.
6. Nataraja, M.C., Dhang, N., and Gupta, A.P., Stress-Strain Curves for Steel-Fiber Reinforced Concrete under Compression, *Cement and Concrete Composites*, 1999.
7. Ramadoss, P., Li., L., Fatima, S., and Sofi, M., Mechanical Performance and Numerical Simulation of High-Performance Steel Fiber Reinforced Concrete, *Journal of Building Engineering*, *64*(October 2022), 2023.
8. Thomas J. and Ramaswamy, A., Mechanical Properties of Steel Fiber-Reinforced Concrete, *Journal of Materials in Civil Engineering*, *19*(5), 2007, pp. 385–392.

9. Furlan S. and De Hanai, J.B., Shear Behaviour of Fiber Reinforced Concrete Beams, *Cement and Concrete Composites*, *19*(4), 1997, pp. 359–366.
10. Mansur, M.A., Ong, K.C.G., and Paramasivam, P., Shear Strength of Fibrous Concrete Beams without Stirrups, *Journal of Structural Engineering*, *112*(9), 1986, pp. 2066–2079.
11. Campione G. and Mangiavillano, M.L., Fibrous Reinforced Concrete Beams in Flexure: Experimental Investigation, Analytical Modelling and Design Considerations, *Engineering Structures*, *30*(11), 2008, pp. 2970–2980.
12. Choi, K.K., Park, H.G., and Wight, J.K., Shear Strength of Steel Fiber-Reinforced Concrete Beams without Web Reinforcement, *ACI Structural Journal*, *104*(1), 2007, pp. 12–21.
13. Mindess, S. and Zhang, L., Impact Resistance of Fibre-Reinforced Concrete, *Proceedings of the Institution of Civil Engineers: Structures and Buildings*, *162*(1), 2009, pp. 69–76.
14. Slater, E., Moni, M., and Alam, M.S., Predicting the Shear Strength of Steel Fiber Reinforced Concrete Beams, *Construction and Building Materials*, *26*(1), 2012, pp. 423–436.
15. Gholamhoseini A., Khanlou, A., MacRae, G., Scott, A., Hicks, S., and Leon, R., An Experimental Study on Strength and Serviceability of Reinforced and Steel Fibre Reinforced Concrete (SFRC) Continuous Composite Slabs, *Engineering Structures*, *114*, 2016, pp. 171–180.
16. Watts, M.J., Amin, A., Gilbert, I.R., Kaufmann, W., and Minelli, F., Simplified Prediction of the Time Dependent Deflection of SFRC Flexural Members, *Materials and Structures/Materiaux et Constructions*, *53*(3), 2020.
17. Khaloo, A.R. and Afshari, M., Flexural Behaviour of Small Steel Fibre Reinforced Concrete Slabs, *Cement and Concrete Composites*, *27*(1), 2005, pp. 141–149.
18. Salehian, H., Barros, J.A.O., and Taheri, M., Evaluation of the Influence of Post-Cracking Response of Steel Fibre Reinforced Concrete (SFRC) on Load Carrying Capacity of SFRC Panels, *Construction and Building Materials*, *73*, 2014, pp. 289–304.
19. Abdul-Ahad, R.B. and Aziz, O.Q., Flexural Strength of Reinforced Concrete T-Beams with Steel Fibers, *Cement and Concrete Composites*, 21(4), 1999, pp. 263–268.
20. Meda, A., Minelli, F., and Plizzari, G.A., Flexural Behaviour of RC Beams in Fibre Reinforced Concrete, *Composites Part B: Engineering*, *43*(8), 2012, pp. 2930–2937.
21. Abbas, A.A., Syed Mohsin, S.M., and Cotsovos, D.M., A Simplified Finite Element Model for Assessing Steel Fibre Reinforced Concrete Structural Performance, *Computers & Structures*, *173,* 2016, pp. 31–49.
22. Beshara, F.B.A. Mustafa, T.S., Mahmoud, A.A., and Khalil, M.M.A., Constitutive Models for Nonlinear Analysis of SFRC Corbels, *Journal of Building Engineering*, *28,* 2020, pp. 101092.
23. Campione, G., Simplified Flexural Response of Steel Fiber-Reinforced Concrete Beams, *Journal of Materials in Civil Engineering*, *20*(4), 2008, pp. 283–293.
24. Campione, G., Flexural Behavior of Steel Fibrous Reinforced Concrete Deep Beams, *Journal of Structural Engineering*, *138*(2), 2012, pp. 235–246.
25. Ferreira, D. and Manie, J., eds., *DIANA User's Manual Release 104*, *DIANA FEA bv*, (2020).
26. Selby, R.G. and Vecchio, F.J., A Constitutive Model for Analysis of Reinforced Concrete Solids, *Canadian Journal of Civil Engineering*, 24, 1997, pp. 460–470.
27. Abbass, W., Khan, M.I., and Mourad, S., Evaluation of Mechanical Properties of Steel Fiber Reinforced Concrete with Different Strengths of Concrete, *Construction and Building Materials*, *168,* 2018, pp. 556–569.
28. De Nicolo, B., Pani, L., and Pozzo, E., Strain of Concrete at Peak Compressive Stress for A Wide Range of Compressive Strengths, *Materials and Structtures*, *27*(4), 1994, pp. 206–210.
29. Lok, T.S. and Xiao, J.R., Flexural Strength Assessment of Steel Fiber Reinforced Concrete, *Journal of Materials in Civil Engineering*, *11*(3), 1999, pp. 188–196.
30. Seo, J., Lee, J., and Lopez, M.M., Parametric Study on Shear Performance for Steel Fiber Reinforced Concrete Beams, *Advances in Structural Engineering*, *18*(7), 2015, pp. 1115–1127.
31. Popovics, S., A Numerical Approach to the Complete Stress-Strain Curve of Concrete, *Cement and Concrete Research*, *3*, 1973, pp. 583–599.
32. Kytinou, V.K., Chalioris, C., and Karayannis, C., Analysis of Residual Flexural Stiffness of Steel Fiber-Reinforced Concrete Beams with Steel Reinforcement, *Materials*, *13*(2698), 2020, pp. 1–24.
33. Yang, M., Huang, C., and Wang, J., Characteristics of Stress-Strain Curve of High Strength Steel Fiber Reinforced Concrete under Uniaxial Tension, *Journal Wuhan University of Technology, Materials Science Edition*, *21*(3), 2006, pp. 132–137.
34. Abdul-Razzak, A.A. and Ali, A.A.M., Influence of Cracked Concrete Models on the Nonlinear Analysis of High Strength Steel Fibre Reinforced Concrete Corbels, *Composite Structures*, *93*(9), 2011, pp. 2277–2287.
35. Lin, W.T., Huan, R., Lee, C.L., and Hsu, H.M., Effect of Steel Fiber on the Mechanical Properties of Cement-Based Composites Containing Silica Fume, *Journal of Marine Science and Technology*, *16*(3), 2008, pp. 214–221.

36. Kim, K.S., Lee, D.H., Hwang, J.H., and Kuchma, D.A., Shear Behavior Model for Steel Fiber-Reinforced Concrete Members without Transverse Reinforcements, *Composites Part B: Engineering*, *43*(5), 2012, pp. 2324–2334.
37. Barros J.A.O., Post-cracking Behaviour of Steel Fibre Reinforced Concrete, *Materials and Structures/Materiaux et Constructions*, *38*, 2005, pp. 47–56.
38. Tlemat, H., Pilakoutas, K., and Neocleous, K., Modelling of SFRC using Inverse Finite Element Analysis, *Materials and Structures*, *39*(286), 2006, pp. 221–233.
39. fib Model Code 2010, *Model Code for Concrete Structures*, Federation Internationale du Beton (fib), 2013.
40. Oh, B.H., Lim, D.H., Yoo, S.W., and Kim, E.S., Shear Behaviour and Shear Analysis of Reinforced Concrete Beams Containing Steel Fibres, *Magazine of Concrete Research*, *50*(4), 1998, pp. 283–291.
41. Yoo, D.Y. and Moon, D.Y., Effect of Steel Fibers on the Flexural Behavior of RC Beams with Very Low Reinforcement Ratios, *Construction and Building Materials*, *188,* 2018, pp. 237–254.